

SUPPORTING INFORMATION

New nanostructured ion-conductive bent-core liquid crystals containing lithium and sodium salts as soft electrolyte candidates.

Carlota Auria-Soro,^{a,b} Nuria Cruz-Navarro,^{a,b} César L. Folcia,^c Isabel Sobrados,^d Amin Sharifi,^e Alfonso Martínez-Felipe,^{*e} and M. Blanca Ros,^{*a,b}

a. Instituto de Nanociencia y Materiales de Aragón (INMA), CSIC-Universidad de Zaragoza, 50009 Zaragoza, Spain.

b. Departamento de Química Orgánica, Facultad de Ciencias, Universidad de Zaragoza, 50009 Zaragoza, Spain

c. Department of Physics, Faculty of Science and Technology, UPV/EHU, E-48080 Bilbao, Spain

d. Instituto de Ciencia de Materiales de Madrid, Consejo Superior de Investigaciones Científicas (CSIC), E-28049 Madrid, Spain

e. Chemical Processes and Materials Research Group, Just Transition Lab, University of Aberdeen, Aberdeen, AB24 3UE, Scotland, UK.

* Corresponding authors: broos@unizar.es and a.martinez-felipe@abdn.ac.uk

Table of contents:

1. Materials and Methods
2. Synthetic Schemes and Experimental Details of the Synthesis of Bent-core Compounds and Hybrid materials.
3. ¹H-NMR, ¹³C-NMR and FT-IR Spectra of Compounds
4. Thermal and Liquid Crystal Properties of the Materials.
5. X-Ray Diffraction Studies.
6. Dielectric Studies in bulk materials.
7. Self-assembly Studies.

- SECTION S1. Materials and Methods

Materials

Chemical reagents utilized in this research were purchased from Sigma-Aldrich and BLD Pharmatech and were employed without further purification. All organic solvents used for synthesis were acquired from Fisher Scientific. Tetrahydrofuran (THF) was purified by a PureSolv solvent purification system (Innovative Technology Inc.). Dichloromethane (DCM) was dried using sodium chloride and 4 mm glass beads and distilled under an Ar atmosphere. Section 2 elucidates the synthetic procedures and characterization data for the novel compounds. Analytical TLC was performed on 60F 254, 60A-15 μm silica gel polyester plates (Merck). Column chromatography was carried out under flash conditions using 60 Å silica gel (Merck).

Methods and techniques

FT-IR spectra were obtained with a Thermo Nicolet Avatar 360 with KBr pellets. A Bruker Microflex spectrometer, equipped with a 337 nm laser with dithranol as the matrix for MALDI-TOF MS experiments, was employed to acquire mass spectral data. Elemental analysis was conducted on a Perkin-Elmer 2400 CHNS elemental analyzer.

Solution NMR spectra were recorded using a Bruker AV-400 spectrometer, operating at 400 MHz for ^1H and 100.62 MHz for ^{13}C . Chemical shift values are reported in ppm referenced to tetramethylsilane (TMS), with the residual solvent signal serving as an internal standard.

^{13}C CP-MAS-NMR and ^1H MAS-NMR spectra were recorded in a Bruker Avance 400 spectrometer (9.4 T). Powder samples were packed in zirconia rotors. Monodimensional spectra were taken at room temperature while the samples were spinning at 10 kHz around the magic angle ($54^\circ 44'$ with respect to the magnetic field). ^7Li MAS NMR and pulsed-field gradient (PFG) NMR experiments were carried out to study the lithium environment and diffusion behavior in the LiTfO-TEG-10-B1-14 complex.

Initial mesophase identification was conducted through microscopic examination of the textures exhibited by samples placed between two glass slides, utilizing Nikon and Olympus BH-2 polarizing microscopes equipped with Linkam THMS600 hot stage. A DSC TA Instrument Q-2000 system was employed to determine the temperatures and enthalpies of bent-core and their hybrid materials phase transitions via calorimetric measurements. Thermogravimetric analyses were performed using a TA Instruments Q5000IR instrument. Thermal analysis of the commercial lithium and sodium salts was carried out using a TA Instruments Discovery SDT650 simultaneous DSC-TGA analyser. Molecular modelling software (Gaussian) was employed to estimate the molecular dimensions.

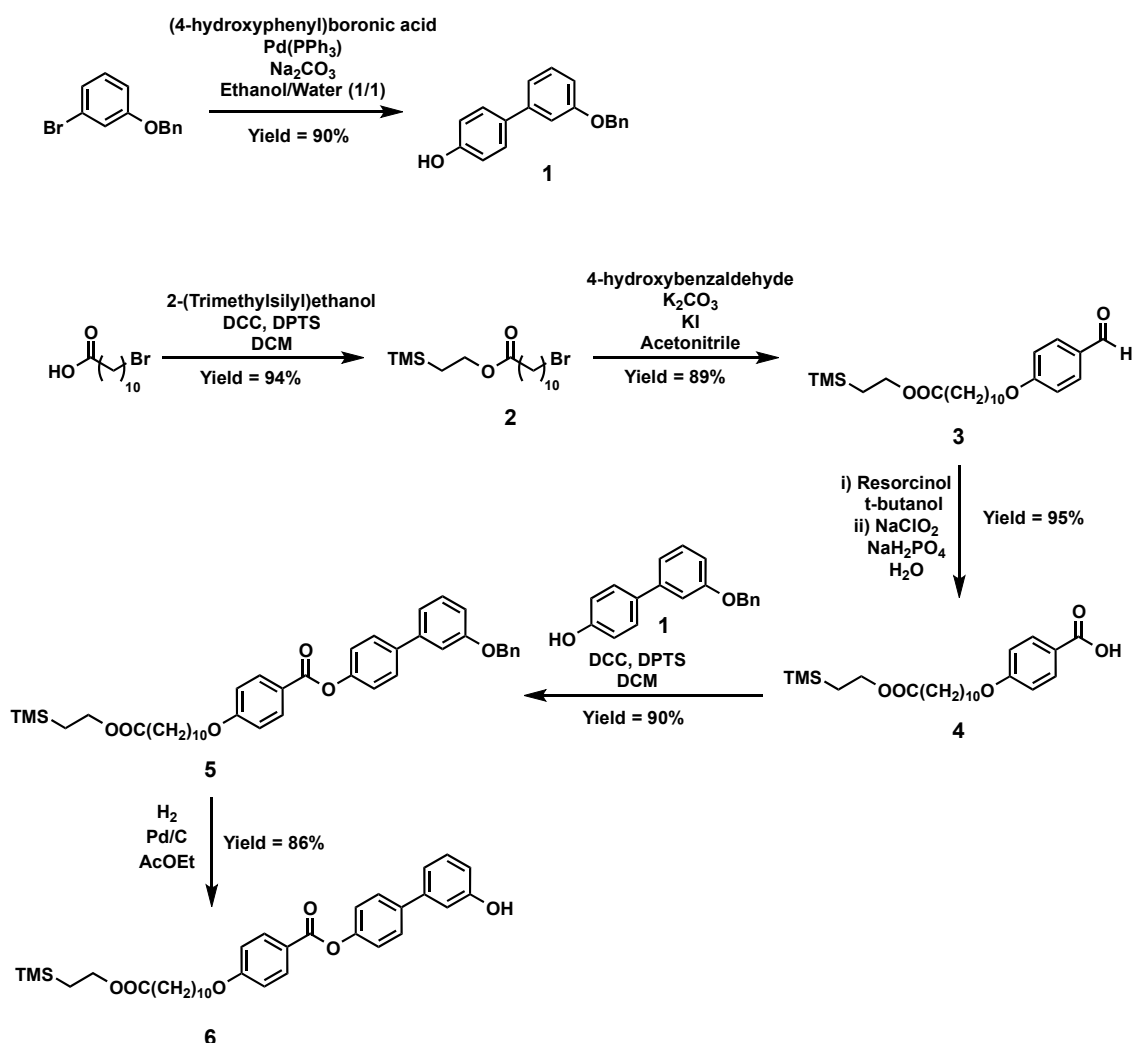
The diffraction diagrams on non-oriented liquid crystal samples were recorded using a Stoe Stadivari goniometer equipped with a Genix3D microfocus generator (Xenocs) and a Dectris Pilatus 100K detector. A specifically designed beam stop device was situated just before the detector allowing high-resolution measurements at angles as small as about 0.7° . Temperature control was achieved using a nitrogen-gas Cryostream controller (Oxford Cryosystems) allowing for temperature control of about 0.1°C . The materials were enclosed in capillary tubes of 0.6 mm of diameter. The exposure time was 5 minutes. Monochromatic Cu-K α radiation ($\lambda = 1.5418 \text{ \AA}$) was used.

For the structural characterization of gels under ambient conditions, a PANalytical Empyrean X-ray diffractometer equipped with a ScatterX78 module was employed. This setup allowed SAXS

analysis starting from 0.08° in 2θ and extending to 78° in WAXS. The samples were placed in 1 mm diameter glass capillaries to maintain structural integrity during 30-minute analysis. PIXcel1D detector, capable of operating in 0D and 1D modes, was used, providing data collection up to 255 times faster than conventional point detectors without compromising data quality. The HighScore software was utilized to optimize sample alignment and positioning. Monochromatic Cu-K α radiation ($\lambda = 1.5418 \text{ \AA}$) was used in all analyses.

Transmission electron microscopy (TEM) was employed to ascertain the morphological characteristics of gel and liquid crystal materials. The analysis was conducted at Advanced Microscopy Laboratory (LMA-UNIZAR) using a TECNAI G20 20 (FEI COMPANY) with an accelerating voltage of 200kV. For sample preparation, a droplet of a dispersion was deposited on a carbon film-coated copper grid. After solvent removal, liquid crystal materials underwent a thermal treatment involving rapid cooling from the liquid phase to room temperature, thereby preserving the mesophase state. Subsequently, a drop of 1% uranyl acetate aqueous solution was applied. After a 30-second interval, excess solution was removed using absorbent paper, with caution exercised to avoid damaging the surface. The samples were then subjected to vacuum drying for 24 hours.

- SECTION S2. Synthetic schemes and experimental details for bent-core compounds and hybrid materials.



Scheme S1. Synthetic route for the preparation of intermediate compounds 1 – 6.

Compound 1¹. In a round bottom flask 1-(benzyloxy)-3-bromobenzene (4.20 g, 15.9 mmol), 4-hydroxyphenyl boronic acid (2 g, 14.5 mmol), K_2CO_3 (2.61 g, 18.9 mmol), and $\text{Pd}(\text{PPh}_3)_4$ (0.84 g, 0.73 mmol) were stirred in EtOH/toluene of 330 mL (1:3, v/v) under Ar atmosphere at 85°C for 5 h. After cooling to the room temperature, the crude was filtered through Celite[®] and the solvent was removed under a reduced pressure. The residue was dissolved in ether and washed with water for several times. After drying over anhydrous MgSO_4 , the solvent was evaporated. The residue was purified by flash column chromatography on silica gel (eluent hexane/dichloromethane 1/1) and recrystallization from hexane to give a white powder. Yield: 3.68 g, 90%.

¹H NMR (400 MHz, CDCl_3): δ (ppm) = 4.74 (s, 1H), 5.12 (s, 2H), 6.87-6.90 (dd, $J=8.70$ Hz, 2H), 6.91-6.94 (m, 1H), 7.13-7.17 (m, 2H), 7.31-7.42 (m, 4H), 7.45-7.48 (m, 4H).

¹³C RMN (100 MHz, CDCl_3): δ (ppm) = 70.55, 113, 49, 113.81, 116.10, 119.84, 128.13, 128.51, 128.86, 129.08, 130.27, 133.98, 137.69, 142.68, 155.94, 159.77.

FTIR (KBr, cm^{-1}): 3366, 3032, 1595, 1526.

Compound 2. 11-Bromoundecanoic acid (5 g, 21.3 mmol), trimethylsilyl ethanol (2.23 g, 18.9 mmol) and DPTS (2.22 g, 7.54 mmol) were dissolved in 50 mL of dry dichloromethane under Ar atmosphere. After cooling in an ice bath, DCC (5.84 g, 28.3 mmol) was slowly added, and the mixture is allowed to react for 24 hours at room temperature. After working up, the crude was filtered, and the solvent was evaporated. The purification was poured on silica gel by flash column chromatography (eluent hexane/dichloromethane 7/3) to obtain a yellow oil. Yield: 4.78 g, 94%.

¹H NMR (400 MHz, CDCl₃): δ (ppm) = 0.04 (s, 9H), 0.94-1.00 (m, 2H), 1.25-1.33 (m, 10H), 1.37-1.45 (m, 2H), 1.56-1.64 (m, 2H), 1.84 (q, J=8.03 Hz, J=6.92 Hz, 2H), 2.27 (t, J=7.54 Hz, 2H), 3.4 (t, J=6.87 Hz, 2H), 4.13-4.17 (m, 2H).

¹³C RMN (100 MHz, CDCl₃): δ (ppm) = 0.02, 18.6, 26.4, 30.2, 30.6, 30.7, 30.80, 30.83, 34.3, 35.4, 36.0, 63.9, 175.5.

FTIR (KBr, cm⁻¹): 2925, 2850, 1725, 1465, 1250.

Compound 3. In a round bottom flask, compound **2** (4.20 g, 11.5 mmol), benzyl 4-hydroxybenzoate (1.68 g, 13.8 mmol), K₂CO₃ (7.94 g, 57.5 mmol), and potassium iodide (0.95 g, 5.80 mmol) were stirred to react under Ar atmosphere at the reflux temperature in 80 mL of acetonitrile overnight. After cooling to room temperature, the solvent was evaporated. The residue was dissolved in ethyl acetate and washed with water and brine. After dried with MgSO₄, the solvent was removed under a reduced pressure. Then the crude product was purified by recrystallization from ethanol to obtain a white solid. Yield: 4.16 g, 89%.

¹H NMR (400 MHz, CDCl₃): δ (ppm) = 0.04 (s, 9H), 0.94-1.01 (m, 2H), 1.26-1.39 (m, 10H), 1.42-1.49 (m, 2H), 1.57-1.65 (m, 2H), 1.77-1.84 (q, J=6.69 Hz, 2H), 2.27 (t, J=7.53 Hz, 2H), 4.03 (t, J=6.55 Hz, 2H), 4.13-4.17 (m, 2H), 6.99 (dd, J=8.71 Hz, 2H), 7.83 (d, J=8.75 Hz, 2H), 9.87 (s, 1H).

¹³C RMN (100 MHz, CDCl₃): δ (ppm) = 1.21, 17.53, 25.18, 25.96, 29.05, 29.14, 29.23, 29.30, 29.35, 29.43, 34.48, 62.62, 68.45, 114.59, 129.78, 132.03, 174.02, 190.77.

FTIR (KBr, cm⁻¹): 2935, 2856, 1729, 1683, 1607, 1575.

Compound 4. In a flask compound **3** (3.50 g, 8.61 mmol) and resorcinol (1.52 g, 13.8 mmol) were dissolved in 180 mL of tert-BuOH at 35°C. A solution of NaClO₂ (4.90 g, 54.2 mmol) and NaH₂PO₄ (4.13 g, 34.4 mmol) in 70 mL of water was slowly added and allowed to react for 24 hours. Afterward, the solvent was evaporated, the solid was redispersed in distilled water, and 2M HCl is added until pH= 1 were reached. The aqueous phase was extracted with ethyl acetate. The organic phase was then washed with water, dried over MgSO₄ and the solvent evaporated. Finally, the residue was purified by recrystallization from ethanol to obtain a white solid. Yield: 3.85 g, 95%.

¹H NMR (400 MHz, CDCl₃): δ (ppm) = 0.04 (s, 9H), 0.95-1.01 (m, 2H), 1.30 (m, 10H), 1.42-1.50 (m, 2H), 1.58-1.65 (m, 2H), 1.77-1.84 (q, J= 6.66 Hz, 2H), 2.27 (t, J=7.54 Hz, 2H), 3.98 (t, J=6.55 Hz, 2H), 4.14-4.18 (m, 2H), 6.91-6.85 (d, J=8.94 Hz, 2H), 8.03-8.06 (d, J=8.91 Hz, 2H).

¹³C RMN (100 MHz, CDCl₃): δ (ppm) = 0.03, 19.01, 26.13, 27.45, 30.57, 30.63, 30.73, 30.80, 30.84, 30.94, 36.02, 63.87, 69.92, 115.84, 122.84, 133.77, 165.24, 173.33, 175.90.

FTIR (KBr, cm⁻¹): 3435, 2935, 2862, 1731, 1679, 1609, 1577, 1255, 1167.

Compound 5. Compound **1** (3.50 g, 8.28 mmol), compound **4** (2.28 g, 8.28 mmol) and DPTS (0.97 g, 3.31 mmol) were dissolved in 25 mL of dry dichloromethane under Ar atmosphere. After cooling in an ice bath, DCC (2.56 g, 12.4 mmol) was slowly added, and the mixture is allowed to react for 24 hours at room temperature. After this time, the crude was filtered, and the solvent was evaporated. The purification was poured on silica gel by flash column chromatography (eluent hexane/dichloromethane 1/1) and recrystallization from ethanol to obtain a white solid. Yield: 5.06 g, 90%.

$^1\text{H NMR}$ (400 MHz, CD_2Cl_2): δ (ppm) = 0.04 (s, 9H), 0.95-1.01 (m, 2H), 1.26-1.41 (m, 10H), 1.44-1.50 (m, 2H), 1.56-1.64 (m, 2H), 1.78-1.85 (q, $J=6.64$ Hz, 2H), 2.26 (t, $J=7.51$ Hz, 2H), 4.06 (t, $J=6.54$ Hz, 2H), 4.11-4.16 (m, 2H), 5.14 (s, 2H), 6.96-6.98 (m, 1H), 6.97-7.02 (d, $J=8.90$ Hz, 2H), 7.21-7.24 (m, 2H), 7.25-7.29 (d, $J=8.63$ Hz, 2H), 7.32-7.43 (m, 4H), 7.46-7.49 (m, 2H), 7.63-7.66 (d, $J=8.67$ Hz, 2H), 8.12-8.16 (d, $J=8.96$ Hz, 2H).

$^{13}\text{C RMN}$ (100 MHz, CD_2Cl_2): δ (ppm) = 1.29, 26.50, 29.91, 34.96, 37.55, 38.17, 66.8, 67.9, 70.3, 113.93, 114.90, 115.58, 120.31, 122.70, 128.14, 128.60, 129.12, 132.28, 132.71, 138.52, 152.00, 152.11, 164.68, 167.87, 177.51.

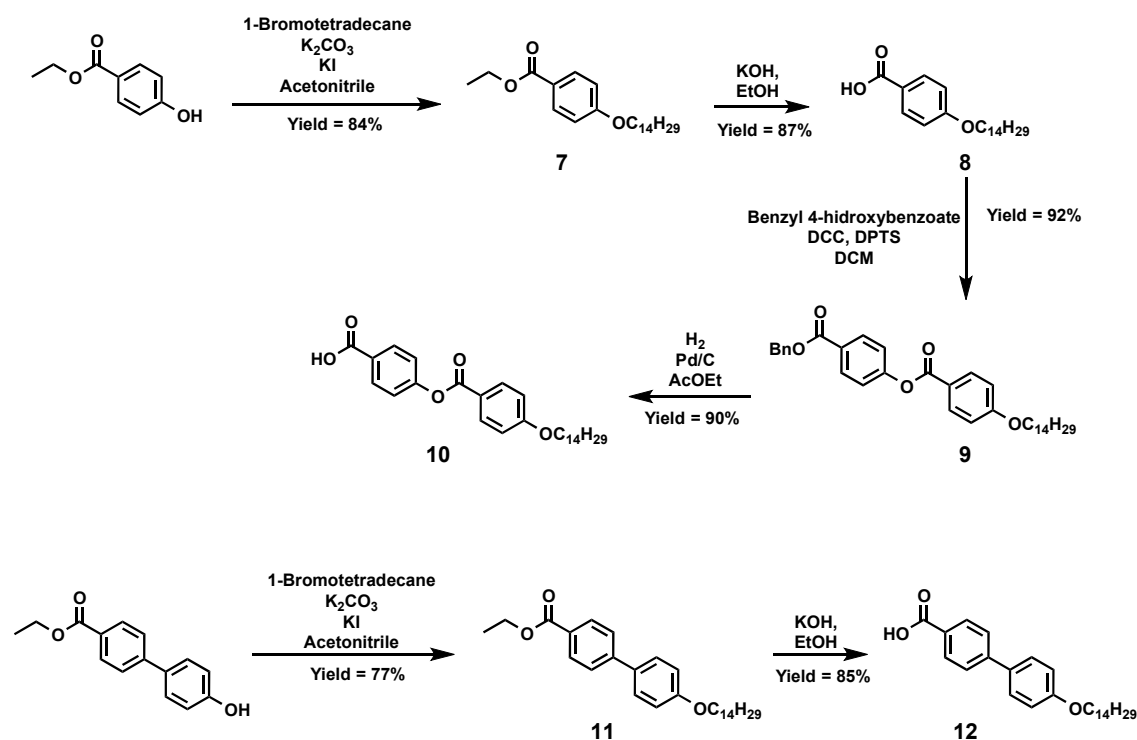
FTIR (KBr, cm^{-1}): 3054, 32932, 2855, 1734, 1606, 1511.

Compound 6. In a round flask compound **5** (4.50 g, 6.61 mmol) and Pd/C (10 wt.%) were stirred in 100 mL of ethyl acetate under hydrogen gas overnight at room temperature. Afterwards, the catalyst was removed by filtration through Celite[®] and the solvent was removed under a reduced pressure. The crude product was recrystallized by ethanol to obtain a white solid. Yield: 3.74 g, 86%.

$^1\text{H NMR}$ (400 MHz, CD_2Cl_2): δ (ppm) = 0.04 (s, 9H), 0.95-1.01 (m, 2H), 1.26-1.41 (m, 10H), 1.44-1.50 (m, 2H), 1.56-1.64 (m, 2H), 1.78-1.85 (q, $J=6.64$ Hz, 2H), 2.26 (t, $J=7.51$ Hz, 2H), 4.06 (t, $J=6.54$ Hz, 2H), 4.11-4.16 (m, 2H), 5.14 (s, 2H), 6.96-6.98 (m, 1H), 6.97-7.02 (d, $J=8.90$ Hz, 2H), 7.21-7.24 (m, 2H), 7.25-7.29 (d, $J=8.63$ Hz, 2H), 7.32-7.43 (m, 4H), 7.46-7.49 (m, 2H), 7.63-7.66 (d, $J=8.67$ Hz, 2H), 8.12-8.16 (d, $J=8.96$ Hz, 2H).

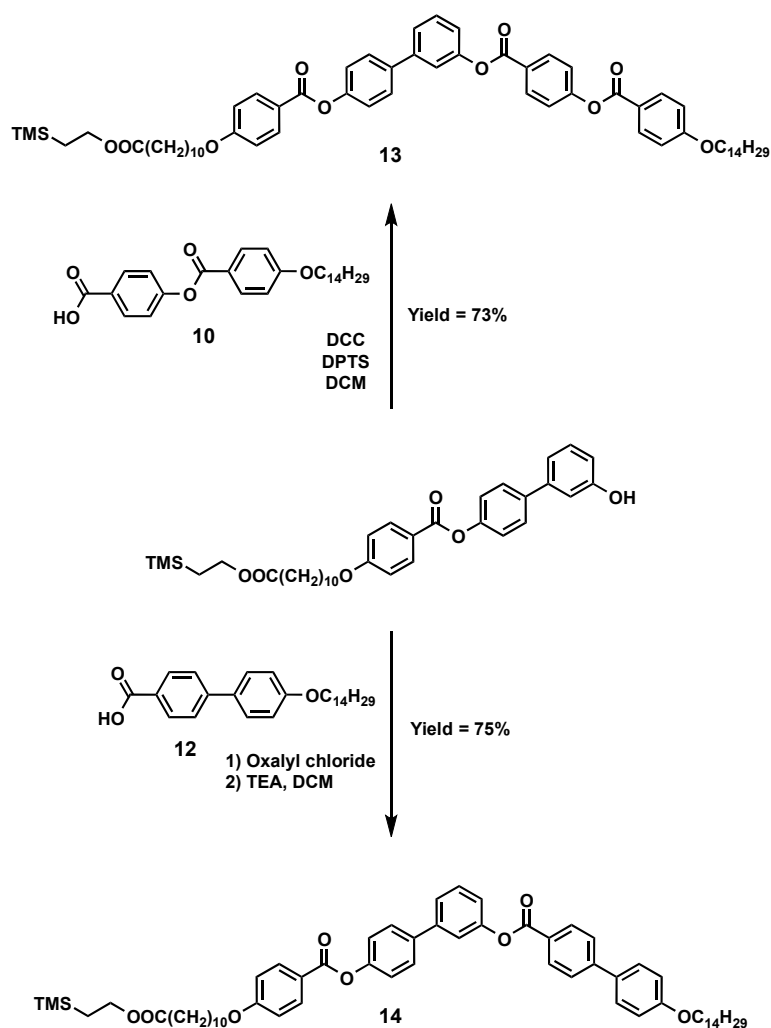
$^{13}\text{C RMN}$ (100 MHz, CD_2Cl_2): δ (ppm) = 1.36, 17.73, 24.32, 26.49, 29.64, 34.96, 62.72, 68.92, 114.44, 114.90, 120.03, 122.72, 128.62, 130.54, 138.71, 143.84, 149.85, 156.72, 158.55, 164.22, 165.42.

FTIR (KBr, cm^{-1}): 3363, 2935, 2858, 1734, 1703, 1609, 1515, 1463.



Scheme S2. Synthetic route for the preparation of intermediate compounds **7 - 12**.

Compounds **7 - 12** were performed as previously described^{2,3}, and since the characterization data aligns with prior publications, experimental details have been omitted.



Scheme S3. Synthetic route for the preparation of intermediate compounds **13** and **14**.

Compound 13. In a flask, compound **6** (1.36 g, 2.30 mmol), compound **10** (1.15 g, 2.53 mmol), DCC (0.71 g, 3.45 mmol) and DPTS (0.20 g, 0.69 mmol) were added in 12 mL of dry dichloromethane, at 0°C and under Ar atmosphere. The mixture was stirred overnight at an ambient temperature. After working up, the crude was filtered, and the solvent was evaporated. The residue was purified by flash column chromatography (eluent hexane/dichloromethane 8/2) to give a white powder- Yield: 1.72 g, 73%.

¹H NMR (400 MHz, CD₂Cl₂): δ (ppm) = 0.04 (s, 9H), 0.86-0.91 (m, 3H), 0.94-1.02 (m, 2H), 1.27-1.4 (m, 10H), 1.43-1.51 (m, 4H), 1.57-1.64 (m, 2H), 1.82 (q, J=13.71 Hz, J=7.06 Hz, 4H) 2.26 (t, J=7.52 Hz, 2H), 4.06 (td, J=6.58 Hz, J=2.00 Hz, 4H), 4.11-4.17 (m, 2H), 6.98-7.04 (dd, J=8.96 Hz, J=3.05 Hz, 2H), 6.98-7.02 (dd, J=8.94 Hz, 2H), 7.22-7.26 (m, 1H), 7.29-7.33 (d, J=8.64 Hz, 2H), 7.38-7.43 (d, J=8.75 Hz, 2H), 7.49-7.59 (m, 3H), 7.67-7.72 (d, J=8.67 Hz, 2H), 8.12-8.17 (dd, J=8.97 Hz, J=2.04 Hz, 4H), 8.28-8.33 (d, J=8.76 Hz, 2H).

¹³C RMN (100 MHz, CD₂Cl₂): δ (ppm) = 14.43, 17.80, 23.23, 25.55, 26.48, 29.66, 29.70, 29.83, 29.90, 29.93, 29.96, 30.06, 30.14, 30.17, 30.23, 30.25, 30.27, 32.51, 39.98, 62.67, 68.87, 114.89, 114.97, 120.92, 121.26, 121.52, 121.96, 122.74, 122.86, 125.19, 127.49, 128.66, 130.40, 132.23, 132.73, 132.85, 138.17, 164.26, 164.49, 164.83, 164.99, 165.38, 174.23.

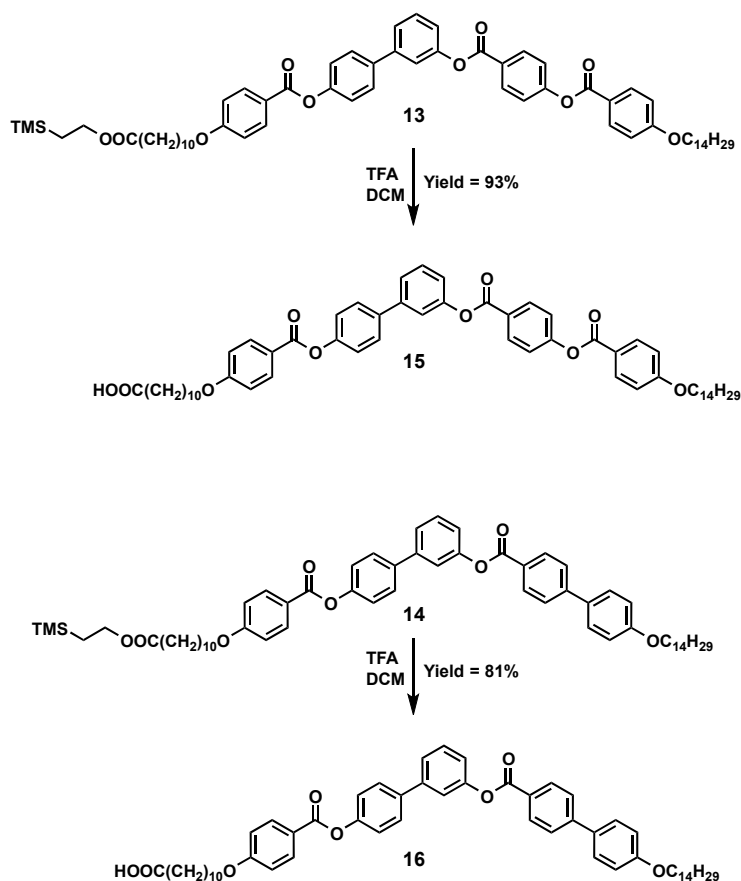
FTIR (KBr, cm⁻¹): 3087, 2934, 2860, 1736, 1605, 1513, 1472, 1256, 1162, 1067.

Compound 14. In a round flask, compound **12** (1.00 g, 2.46 mmol) was dissolved in 10 mL oxalyl chloride under Ar atmosphere at the reflux temperature for 3 hours. After this time, the crude was cooled, and the solvent was removed under a reduced pressure. The precipitated was dissolved in 10 mL of dry dichloromethane and added to a solution of compound **6** (1.21 g, 2.05 mmol) and triethylamine (0.29 g, 2.87 mmol) in 40 mL of dry dichloromethane to react for 24 hours under Ar atmosphere. The crude was filtered, and the solvent was evaporated. The crude product was purified by flash column chromatography on silica gel (eluent hexane/dichloromethane 9/1) to obtain a white powder. Yield: 1.54 g, 75%.

¹H NMR (400 MHz, CD₂Cl₂): δ (ppm) = 0.04 (s, 9H), 0.86-0.90 (m, 3H), 0.95-0.99 (m, 2H), 1.27-1.4 (m, 30H), 1.44-1.52 (m, 4H), 1.56-1.63 (m, 2H), 1.77-1.85 (m, 4H) 2.26 (t, J=7.53 Hz, 2H), 4.00-4.08 (m, 4H), 4.11-4.15 (m, 2H), 6.98-7.03 (dd, J=8.89 Hz, J=2.29 Hz, 4H), 7.23-7.26 (m, 1H), 7.28-7.32 (d, J=8.65 Hz, 2H), 7.49-7.43 (m, 3H), 7.49-7.59 (m, 3H), 7.62-7.66 (d, J=8.83 Hz, 2H), 7.67-7.71 (d, J=8.67 Hz, 2H), 7.73-7.76 (d, J=8.80 Hz, 2H), 8.12-8.16 (d, J=8.90 Hz, 2H), 8.24-8.27 (d, J=8.68 Hz, 2H).

¹³C RMN (100 MHz, CD₂Cl₂): δ (ppm) = 14.37, 17.78, 23.33, 25.54, 26.51, 26.59, 29.67, 29.70, 29.83, 29.90, 29.94, 29.96, 30.06, 30.17, 30.19, 30.24, 30.26, 30.28, 32.50, 34.92, 62.71, 68.75, 69.03, 114.74, 115.47, 120.95, 121.30, 121.95, 122.83, 125.01, 127.06, 128.06, 128.72, 128.89, 130.37, 131.20, 132.25, 132.71, 151.55, 152.20, 160.31, 164.25, 165.33, 165.62, 174.27.

FTIR (KBr, cm⁻¹): 3080, 2928, 2854, 1730, 1605, 1577, 1252, 1172.



Scheme S4. Synthetic route for the preparation of intermediate compounds **15** and **16**.

Compound 15⁴. Compound **13** (1.79 g, 1.74 mmol) was dissolved in 21.8 mL of dry dichloromethane under Ar atmosphere and cooled to ice bath. Then, 21.8 mL of trifluoroacetic acid was slowly added and the mixture was stirred at room temperature for 4 hours. After this time, the acid was neutralized with an excess of water and ice, and the crude extracted with dichloromethane, drying the organic layer over anhydrous MgSO₄. The solvent was removed by evaporation under a reduced pressure and the crude product was recrystallized by ethanol to give a white solid. Yield: 1.50 g, 93%.

¹H NMR (400 MHz, CD₂Cl₂): δ (ppm) = 0.86-0.90 (m, 3H), 1.26-1.41 (m, 30H), 1.44-1.52 (m, 4H), 1.59-1.66 (m, 2H), 1.78-1.86 (m, 4H) 2.35 (t, J=7.53 Hz, 2H), 4.04-4.09 (td, J=6.57 Hz, J=2.66 Hz, 4H), 6.99-7.02 (dd, J=8.94 Hz, J=4.29 Hz, 4H), 7.23-7.26 (m, 1H), 7.29-7.31 (d, J=8.66 Hz, 2H), 7.39-7.41 (d, J=8.74 Hz, 2H), 7.48-7.58 (m, 3H), 7.49-7.59 (m, 3H), 7.67-7.71 (d, J=8.65 Hz, 2H), 8.13-8.16 (dd, J=8.95 Hz, J=2.82 Hz, 4H), 8.29-8.31 (d, J=8.81 Hz, 2H).

¹³C RMN (100 MHz, CD₂Cl₂): δ (ppm) = 14.24, 22.76, 24.84, 26.11, 29.71, 32.02, 33.53, 68.39, 68.63, 114.46, 114.96, 120.54, 121.60, 122.31, 122.72, 123.34, 124.84, 125.46, 128.39, 130.04, 130.51, 131.38, 132.50, 137.77, 142.10, 147.05, 150.71, 155.94, 162.46, 164.77, 177.06.

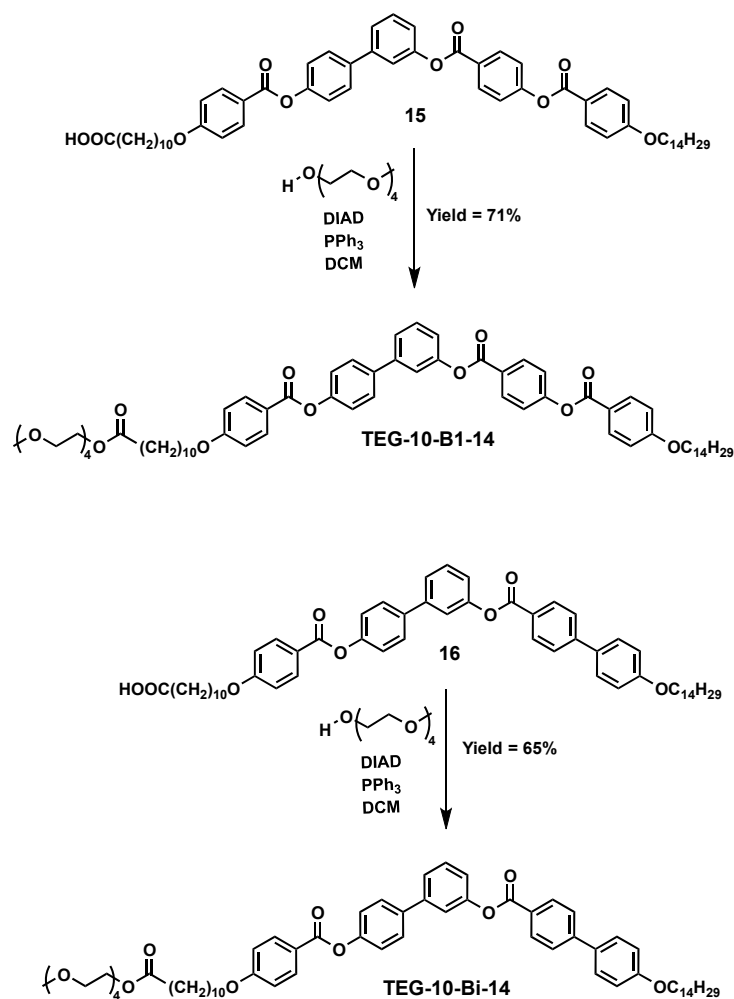
FTIR (KBr, cm⁻¹): 3075, 2923, 2857, 1730, 1601, 1578, 1507, 1471, 1261.

Compound 16. Compound **14** (1.43 g, 1.39 mmol) was dissolved in 17.4 mL of dry dichloromethane under Ar atmosphere and cooled to ice bath. Then, 17.4 mL of trifluoroacetic acid was slowly added and the mixture was stirred at room temperature for 4 hours. After this time, the acid was neutralized with an excess of water and ice, and the crude extracted with dichloromethane, drying the organic layer over anhydrous MgSO₄. The solvent was removed by evaporation under a reduced pressure and the crude product was recrystallized by ethanol to give a white solid. Yield: 0.99 g, 81%.

¹H NMR (400 MHz, CD₂Cl₂): δ (ppm) 0.89-0.93 (m, 3H), 1.28-1.42 (m, 30H), 1.48-1.55 (m, 4H), 1.65-1.72 (m, 2H), 1.81-1.88 (m, 4H), 2.38 (t, J=7.47 Hz, 2H), 4.03-4.10 (m, 4H), 6.99-7.05 (dd, J=11.32 Hz, J=8.87 Hz, 4H), 7.30-7.34 (d, J=8.63 Hz, 2H), 7.49-7.54 (m, 3H), 7.60-7.64 (d, J=8.78 Hz, 2H), 7.66-7.70 (d, J=8.64 Hz, 2H), 7.71-7.75 (d, J=8.54 Hz, 2H), 8.16-8.20 (d, J=8.87 Hz, 2H), 8.27-8.30 (d, J=8.47 Hz, 2H).

¹³C RMN (100 MHz, CD₂Cl₂): δ (ppm) = 14.7, 22.80, 24.86, 26.17, 29.61, 32.09, 33.34, 68.58, 114.46, 115.30, 120.60, 122.18, 124.72, 126.74, 128.53, 129.82, 130.97, 132.44, 138.06, 142.28, 146.32, 148.22, 150.68, 157.51, 163.26, 164.93, 169.78.

FTIR (KBr, cm⁻¹): 3445, 3056, 2921, 2854, 1733, 1602, 1581, 1476, 1293, 1202, 1169, 1090.



Scheme S5. Synthetic route for the preparation of compounds **TEG-10-Bx-14**.

Compounds TEG-10-B1-14. In a round flask, compound **15** (1.00 g, 1.08 mmol), tetraethylglycol monomethyl ether (0.25 g, 1.19 mmol), DCC (0.33 g, 1.62 mmol) and DPTS (0.13 g, 0.43 mmol) in 14 mL of dry dichloromethane under Ar atmosphere and the mixture was stirred overnight at ambient temperature. The crude was filtered and washed with dichloromethane. The filtrate was extracted with dichloromethane/water and the organic layer was dried over anhydrous MgSO₄. The residue was purified by flash column chromatography silica gel (eluent dichloromethane/ethyl acetate 9/1) and recrystallization by ethanol, to obtain a white powder. Yield: 0.86 g, 71%.

¹H NMR (400 MHz, CD₂Cl₂): δ (ppm) = 0.87-0.91 (m, 3H), 1.26-1.37 (m, 30H), 1.44-1.52 (m, 4H), 1.58-1.63 (m, 4H), 1.79-1.86 (m, 4H), 2.33 (t, J=7.53 Hz, 2H), 3.34 (s, 3H), 3.49-3.52 (m, 2H), 3.57-3.60 (m, 10H), 3.64-3.67 (m, 2H), 4.04-4.09 (td, J=6.60 Hz, J=6.58 Hz, J=2.28 Hz, 4H), 4.18-4.21 (m, 2H), 6.99-7.03 (dd, J=8.95 Hz, J=3.62 Hz, 4H), 7.23-7.26 (m, 1H), 7.30-7.32 (d, J=8.69 Hz, 2H), 7.39-7.42 (d, J=8.76 Hz, 2H), 7.49-7.59 (m, 3H), 7.68-7.70 (d, J=8.71 Hz, 2H).

¹³C RMN (100 MHz, CD₂Cl₂): δ (ppm) = 14.44, 23.28, 25.48, 26.50, 29.66, 29.83, 29.89, 29.93, 29.96, 30.06, 30.13, 30.16, 30.22, 30.25, 30.26, 32.52, 34.67, 59.19, 63.92, 69.00, 69.06, 69.71, 70.96, 71.05, 71.12, 72.46, 114.88, 114.97, 120.95, 121.26, 121.52, 121.98, 122.75, 122.87, 125.14, 127.49, 128.67, 130.38, 132.21, 132.69, 132.86, 138.16, 142.59, 151.62, 152.08, 156.08, 164.22, 164.51, 164.80, 165.00, 165.40, 174.12.

FTIR (KBr, cm⁻¹): 2921, 2854, 1730, 1605, 1476, 1292, 1256, 1198, 1174, 1090.

MALDI-MS (ditranol/TFANa): m/z 1139.61 [M+Na]⁺.

Elemental analysis: Calcd. for C₆₇H₈₈O₁₄ C 72.02, H 7.94; found C 72.53, H 7.82.

Compound TEG-10-Bi-14. In a round flask, compound **16** (0.71 g, 0.80 mmol), tetraethylglycol monomethyl ether (0.19 g, 0.88 mmol), DCC (0.25 g, 1.20 mmol) and DPTS (95 mg, 0.32 mmol) in 10 mL of dry dichloromethane under Ar atmosphere and the mixture was stirred overnight at ambient temperature. The crude was filtered and washed with dichloromethane. The filtrate was extracted with dichloromethane/water and the organic layer was dried over anhydrous MgSO₄. The residue was purified by flash column chromatography silica gel (eluent dichloromethane/ethyl acetate 98/2) and recrystallization by ethanol, to obtain a white powder. Yield: 0.56 g, 65%.

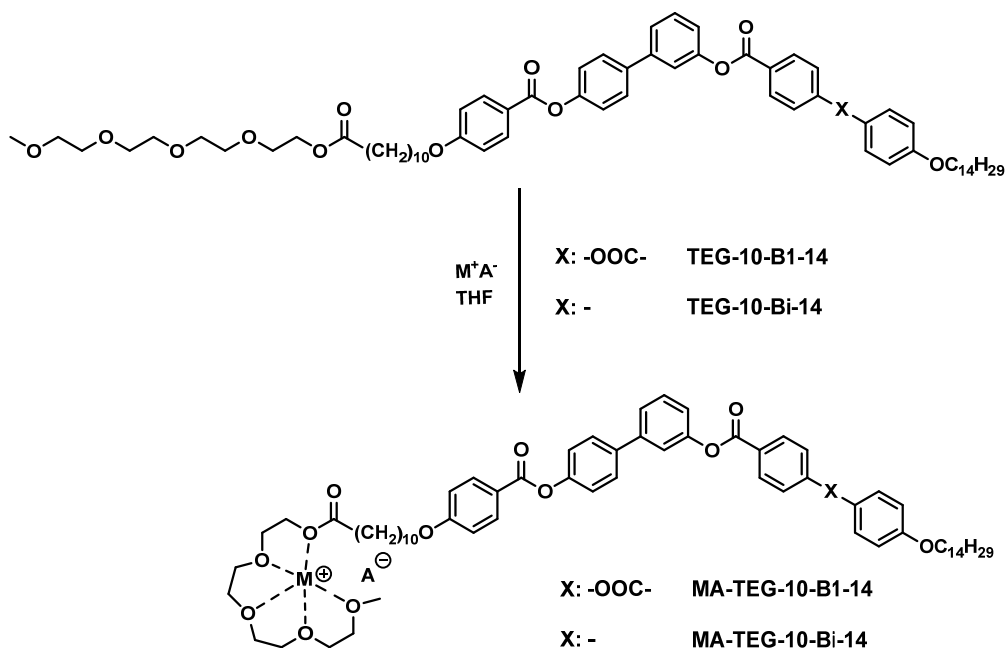
¹H NMR (400 MHz, CD₂Cl₂): δ (ppm) = 0.86-0.90 (m, 3H), 1.27-1.40 (m, 30H), 1.44-1.52 (m, 4H), 1.58-1.64 (m, 4H), 1.77-1.85 (m, 4H), 2.32 (t, J=7.47 Hz, 2H), 3.34 (s, 3H), 3.49-3.52 (m, 2H), 3.56-3.61 (m, 10H), 3.64-3.67 (m, 2H), 4.00-4.07 (td, J=15.05 Hz, J=6.58 Hz, J=6.58 Hz, 4H), 4.18-4.20 (m, 2H), 6.99-7.03 (dd, J=8.88 Hz, J=4.85 Hz, 4H), 7.23-7.26 (m, 1H), 7.29-7.32 (d, J=8.66 Hz, 2H), 7.49-7.58 (m, 3H), 7.63-7.65 (d, J=8.82 Hz, 2H), 7.68-7.70 (d, J=8.68 Hz, 2H), 7.73-7.76 (d, J=8.61 Hz, 2H).

¹³C RMN (100 MHz, CD₂Cl₂): δ (ppm) = 14.43, 23.25, 25.48, 26.48, 26.60, 29.67, 29.82, 29.89, 29.94, 29.96, 30.06, 30.16, 30.18, 30.23, 30.26, 30.27, 32.47, 34.67, 59.20, 63.92, 68.77, 69.00, 69.71, 70.96, 71.05, 71.12, 72.47, 114.82, 115.41, 120.99, 121.34, 121.99, 122.87, 125.04, 127.03, 128.03, 128.68, 128.91, 130.38, 131.13, 132.26, 132.72, 138.19, 142.52, 146.47, 151.51, 152.16, 160.25, 164.24, 165.35, 165.66, 174.12.

FTIR (KBr, cm⁻¹): 2921, 2854, 1733, 1605, 1584, 1472, 1270, 1175.

MALDI-MS (ditranol/TFANa): m/z 1095.62 [M+Na]⁺.

Elemental analysis: Calcd. for C₆₆H₈₈O₁₂ C 73.85, H 8.26; found C 73.92, H 8.09.



Scheme S6. Synthetic route for the preparation of complexes **MA-TEG-10-Bx-14**.

- Preparation of MA-TEG-10-Bx-14 complexes.

The corresponding bent-core TEG-based compounds (**TEG-10-Bx-14**) and the selected cationic salts (LiTfO, LiTf₂N, NaTfO, and NaTf₂N) were dissolved and combined in THF in equimolar proportions (1:1 molar ratio). The resultant solutions were subjected to ultrasonication for 15 minutes to enhance component dissolution and ensure homogeneous mixing. Subsequently, the mixtures underwent slow evaporation under continuous orbital stirring at room temperature to facilitate controlled solvent removal. Finally, the obtained solid residues were further dried under vacuum at 50 °C for 24 hours to eliminate any residual solvent.

Complex formation was checked by ¹H-NMR and FT-IR. Figs. S3 - S5 show representative spectra corresponding to **TEG-10-Bx-14** and **MA-TEG-10-Bx-14** based on 1/1 molar ratios.

- Preparation of physical gels.

The gel preparation process was conducted in shell vials sealed with polyethylene stoppers (40 mm long × 8.2 mm wide, 1.00 mL volume), combining 1 wt% of the gelators with the selected solvents. The mixtures were subsequently heated to a temperature 5 °C below the boiling point of the liquid in an alumina block mold using an electric heating plate equipped with a temperature regulator, ensuring a controlled heating rate of 1 °C min⁻¹ for precise determination of the thermal gel-to-sol transition temperature. Upon achieving complete dissolution, the resulting isotropic solutions were left to cool to room temperature without controlling the cooling rate. Gel formation was assessed using the *vial inversion test*, wherein a sample was categorized as a "gel" if it remained stationary and did not exhibit flow under gravitational force upon vial inversion at ambient temperature.

- SECTION S3. $^1\text{H-NMR}$, $^{13}\text{C-NMR}$ and FT-IR Spectra of Compounds

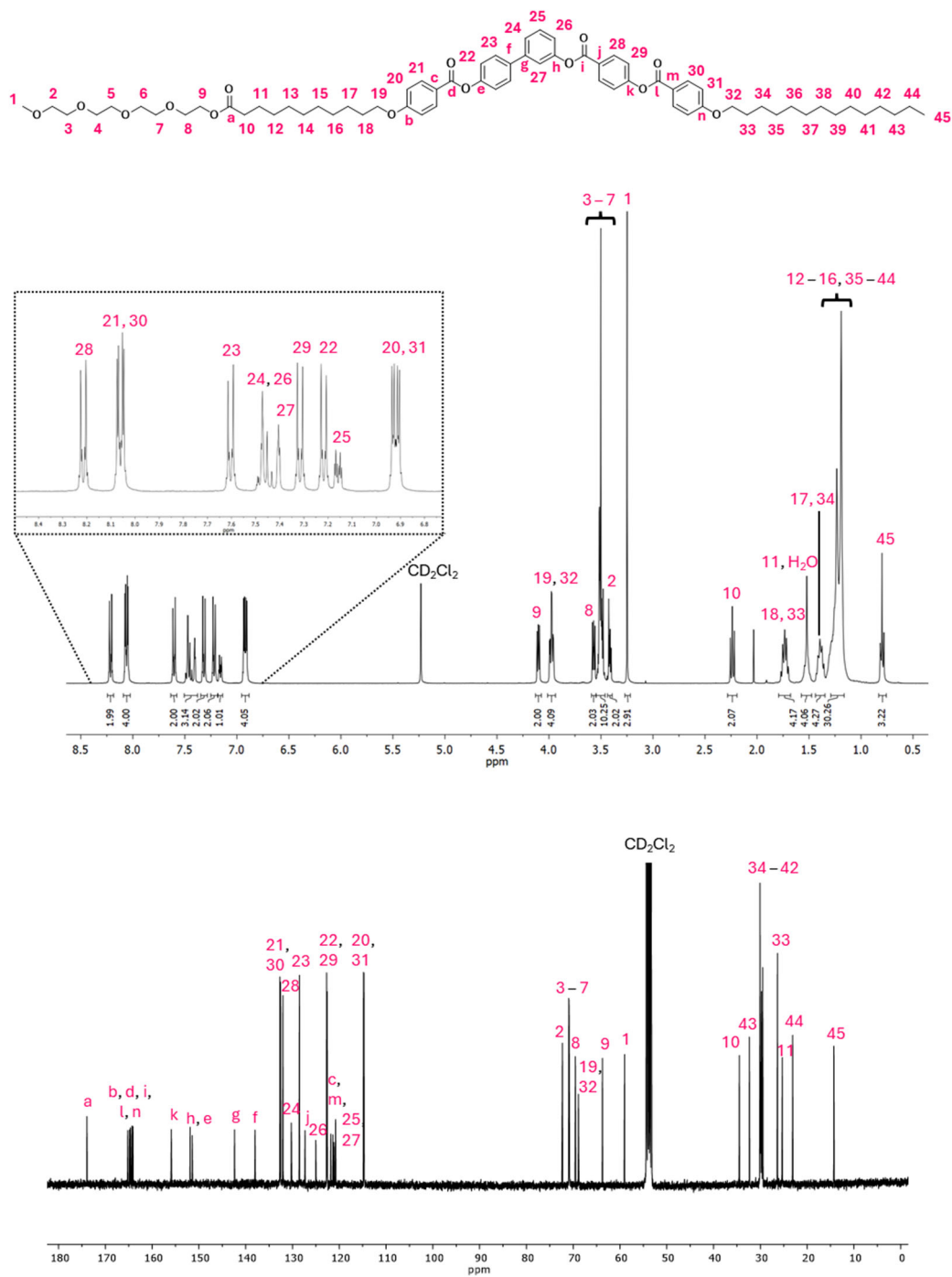


Figure S1. $^1\text{H-NMR}$ and $^{13}\text{C-NMR}$ spectra of TEG-10-B1-14 (CD₂Cl₂, 400MHz).

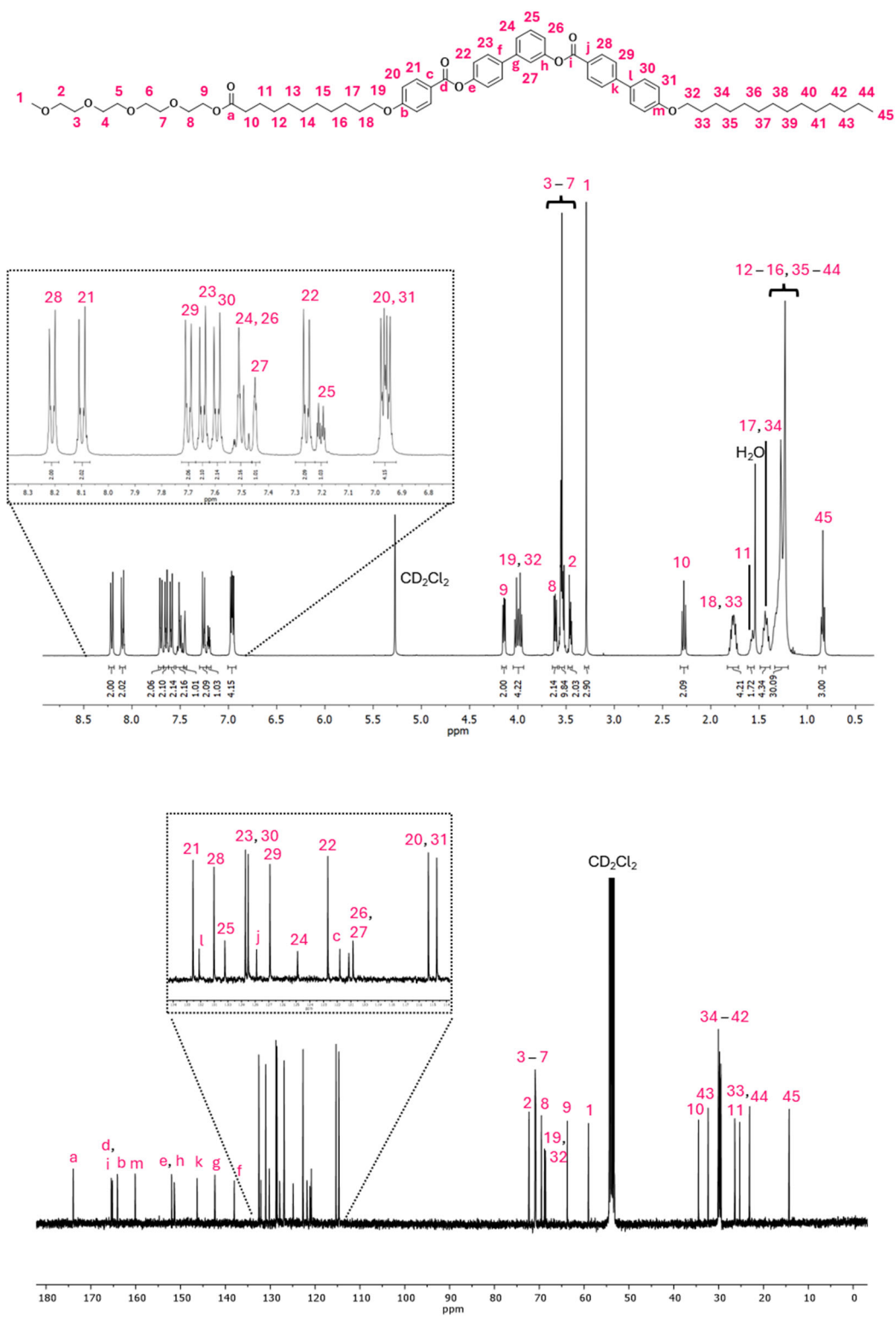


Figure S2. ^1H -NMR and ^{13}C -NMR spectra of TEG-10-Bi-14 (CD_2Cl_2 , 400MHz).

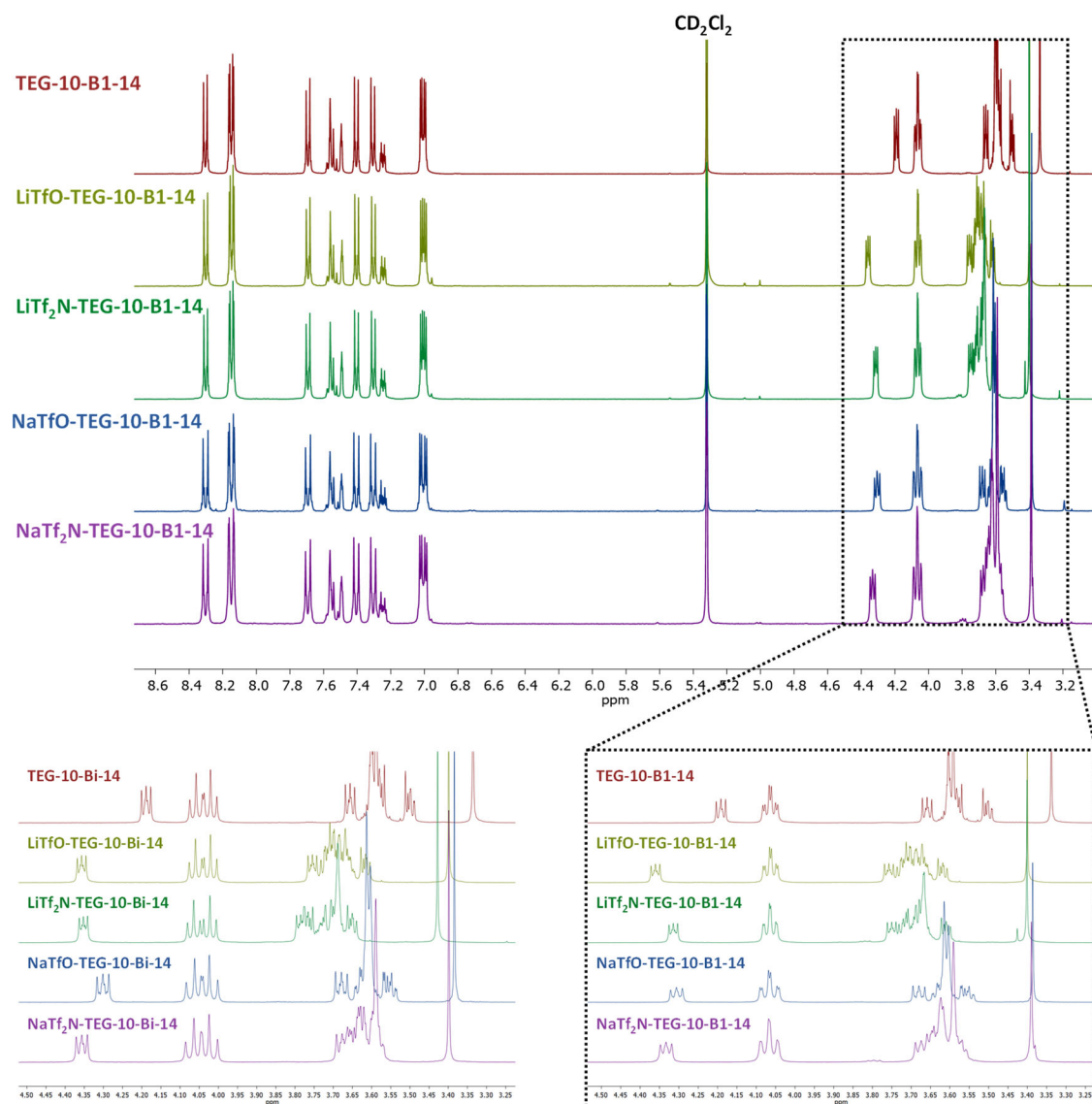


Figure S3. Comparative $^1\text{H-NMR}$ of the region corresponding to the $-\text{CH}_2-\text{CH}_2-\text{O}-$ segment of TEG-10-Bx-14 compounds and MA-TEG-10-B1-14 complexes in solution (CD_2Cl_2 , 400MHz).

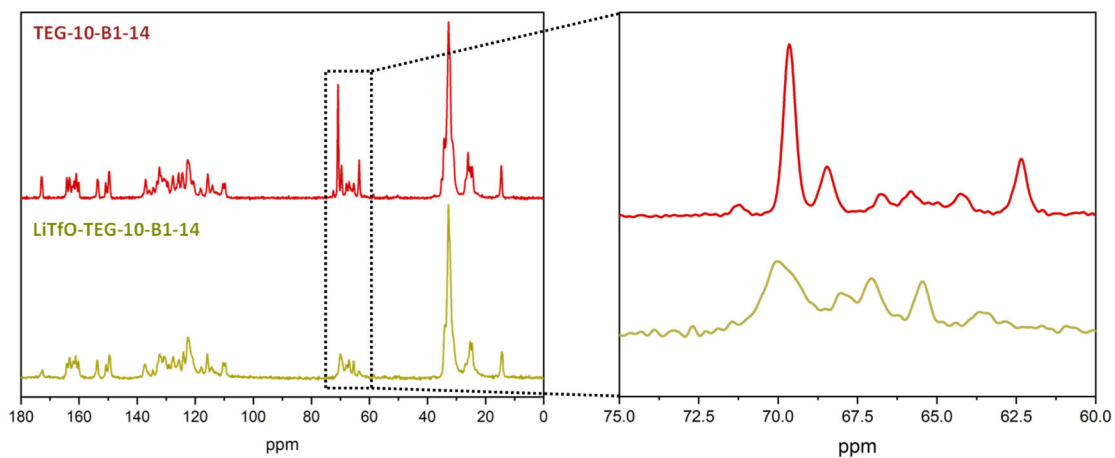


Figure S4. ^{13}C -CP-MAS RMN spectra of **TEG-10-B1-14** and **LiTfO-TEG-10-B1-14**

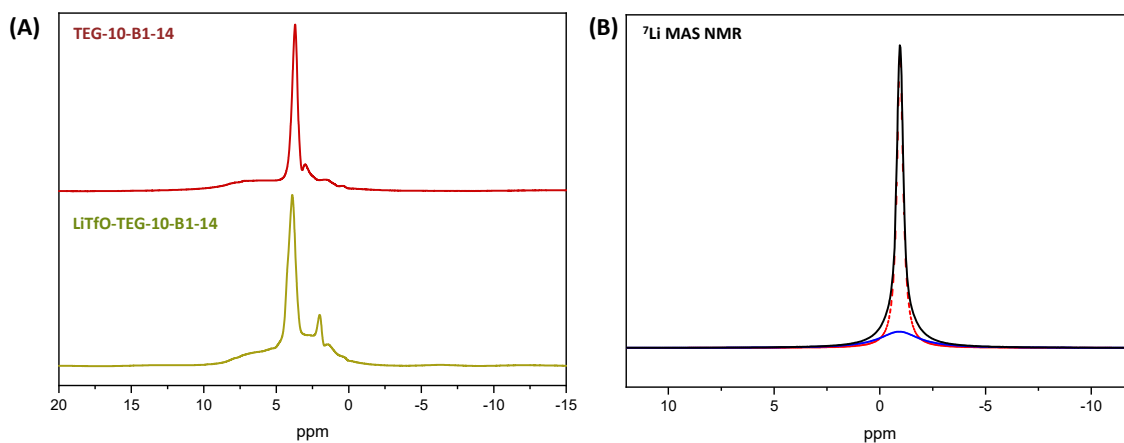


Figure S5. (A) ^1H MAS NMR spectra of **TEG-10-B1-14** and **LiTfO-TEG-10-B1-14** compounds.
(B) ^7Li MAS NMR spectrum of **LiTfO-TEG-10-B1-14** complex.

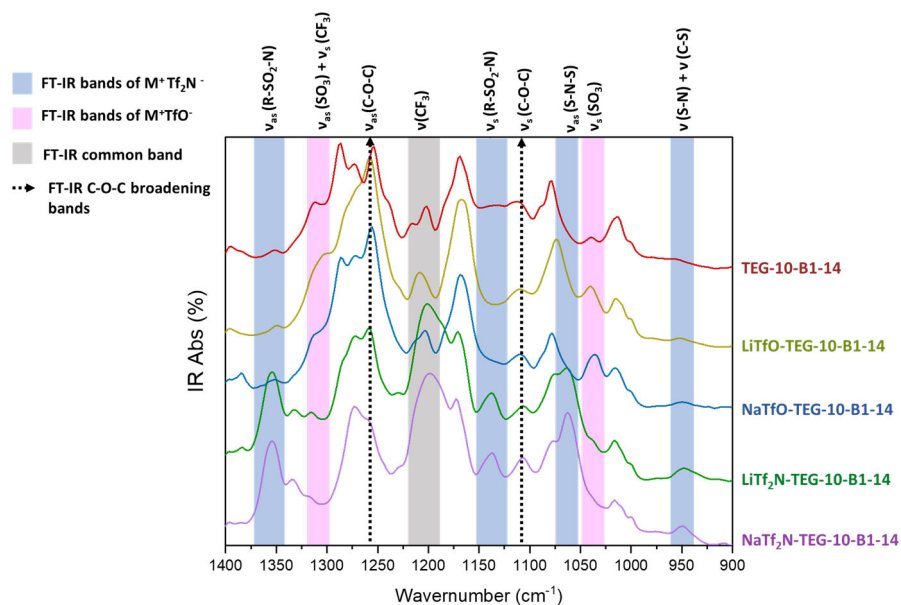


Figure S6. Comparative FT-IR spectra of the $-\text{CH}_2\text{-CH}_2\text{-O}-$ region corresponding to **TEG-10-B1-14** compound and **MA-TEG-10-B1-14** complexes measured at $T=25^\circ\text{C}$ (in KBr).

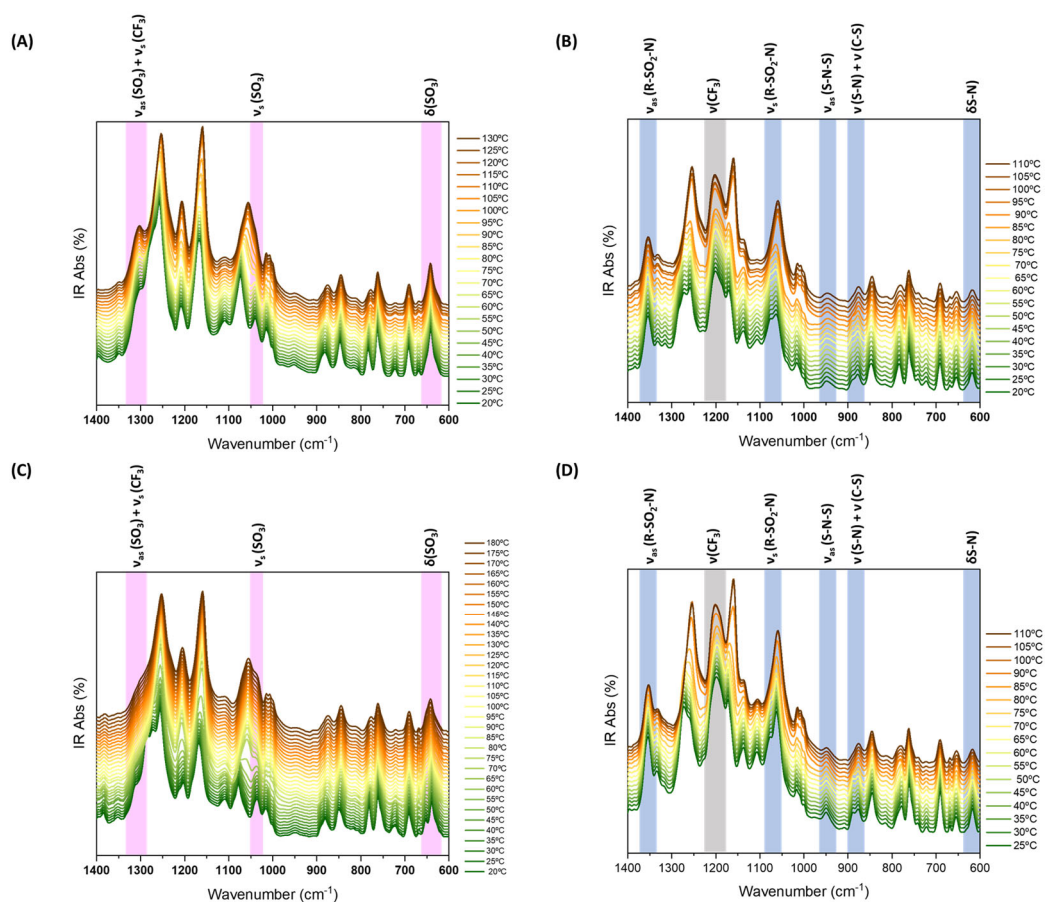


Figure S7. Temperature-dependent FT-IR spectra of complexes; A) **LiTfO-TEG-10-B1-14**, B) **LiTf₂N-TEG-10-B1-14**, C) **NaTfO-TEG-10-B1-14**, and D) **NaTf₂N-TEG-10-B1-14**, respectively, measured at their corresponding range transitions (in KBr). Selective complexation of the ions in TEG region is determined by the appearance of new contributions (coloured squares mark) from the TfO (pink) and Tf₂N (blue) ions.

- SECTION S4. Thermal and Liquid Crystal Properties of the Materials.

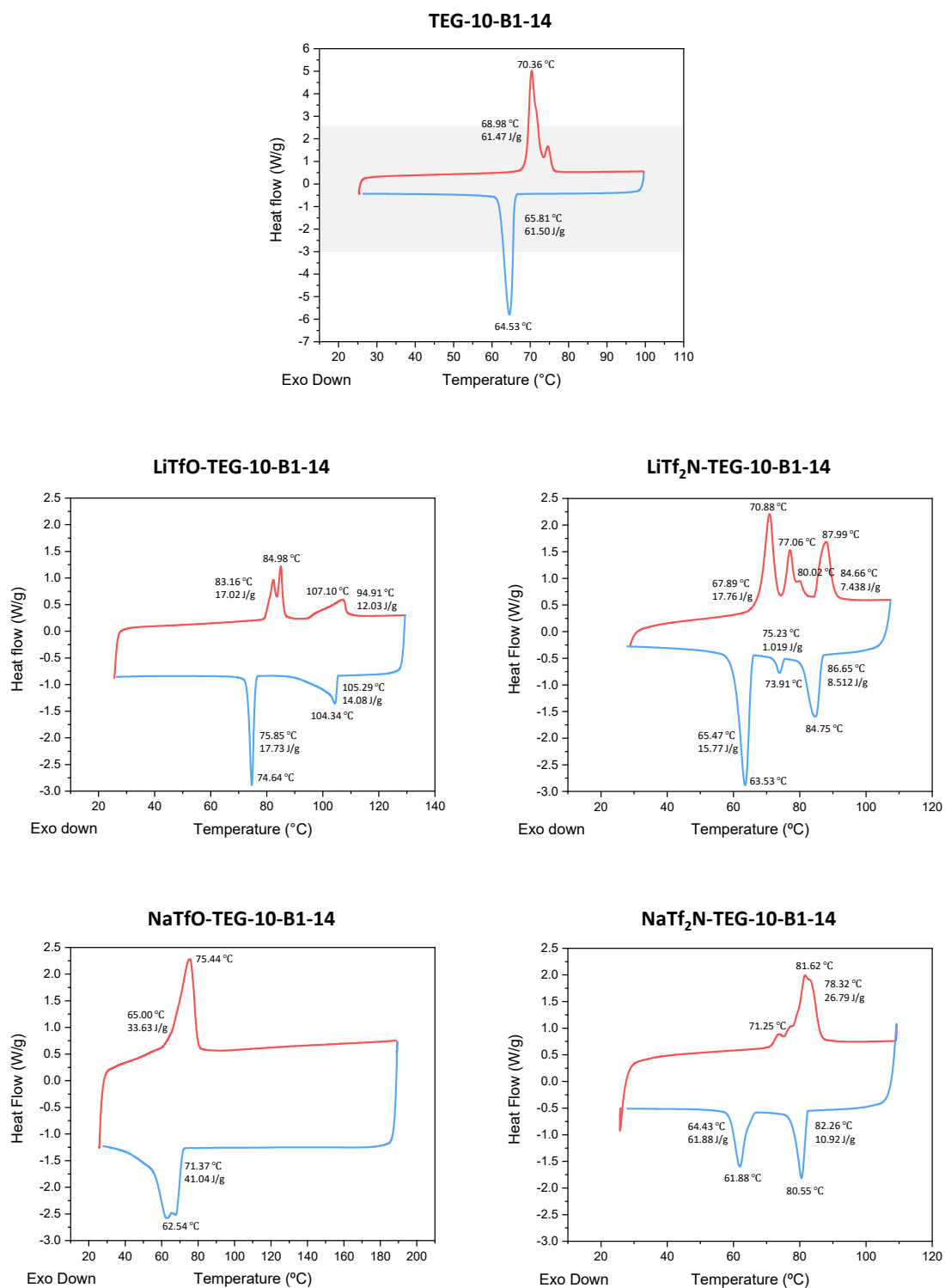
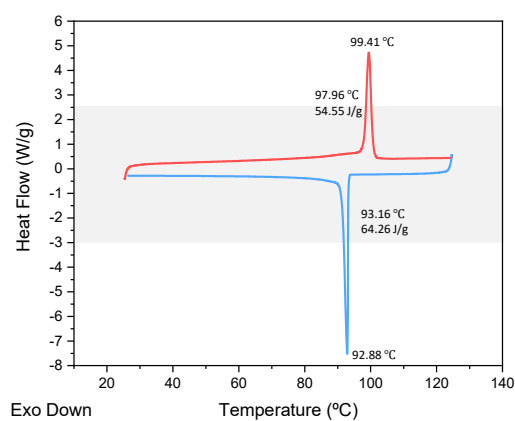
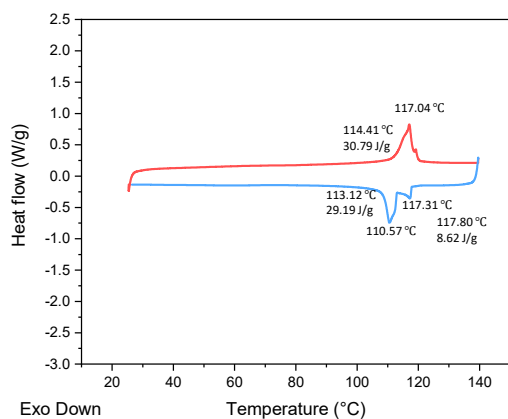


Figure S8. DSC thermograms, second heating (red line)/cooling (blue line) cycles (rate 5 °C min⁻¹) of **TEG-10-B1-14** compound and **MA-TEG-10-B1-14** complexes (grey box mark heat flow, +2.5 and -3 W g⁻¹, for comparative purposes).

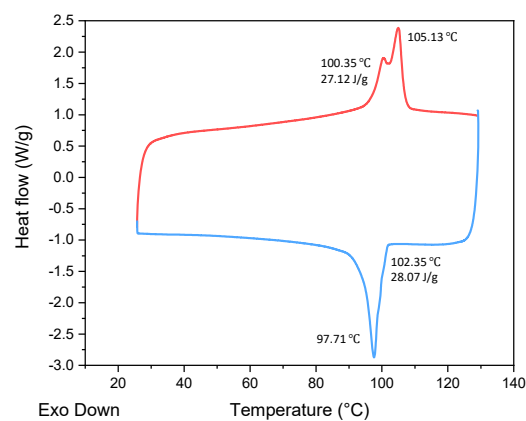
TEG-10-Bi-14



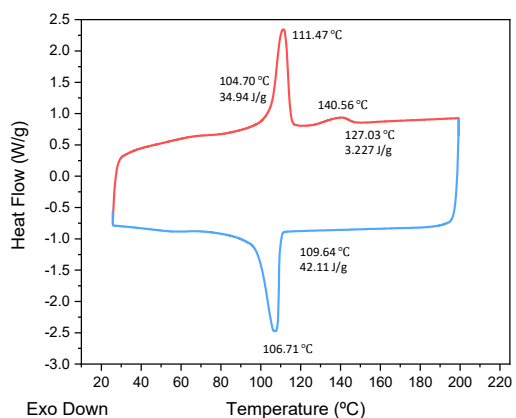
LiTfO-TEG-10-Bi-14



LiTf₂N-TEG-10-Bi-14



NaTfO-TEG-10-Bi-14



NaTf₂N-TEG-10-Bi-14

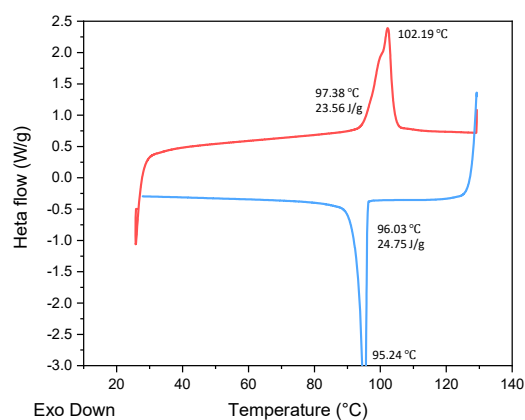


Figure S9. DSC thermograms, second heating (red line)/cooling (blue line) cycles (rate 5 °C min⁻¹) of **TEG-10-Bi-14** compound and **MA-TEG-10-Bi-14** complexes (grey box mark heat flow, +2.5 and -3 W g⁻¹, for comparative purposes).

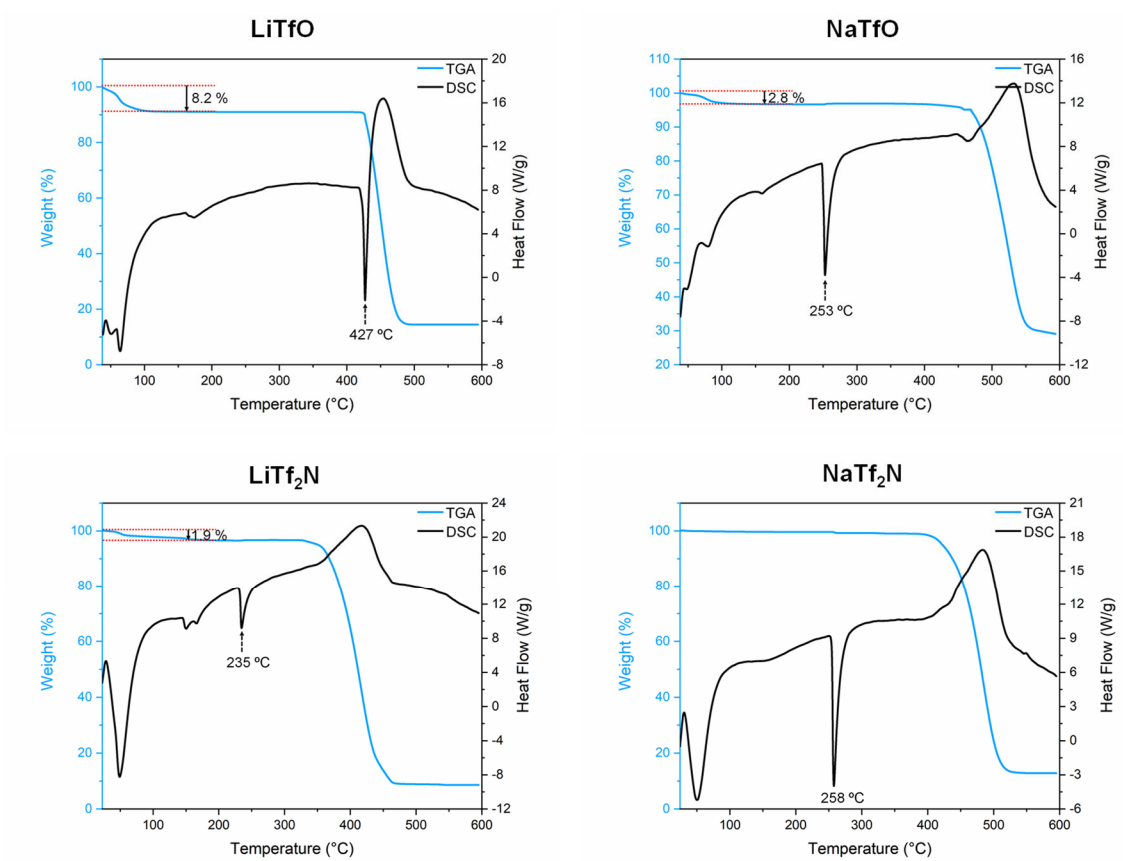


Figure S10. TGA (blue curves) and DSC (black curves) thermograms of commercial virgin samples of LiTfO, NaTfO, LiTf₂N and NaTf₂N, recorded upon heating under inert atmosphere at a rate of 10 °C min⁻¹.

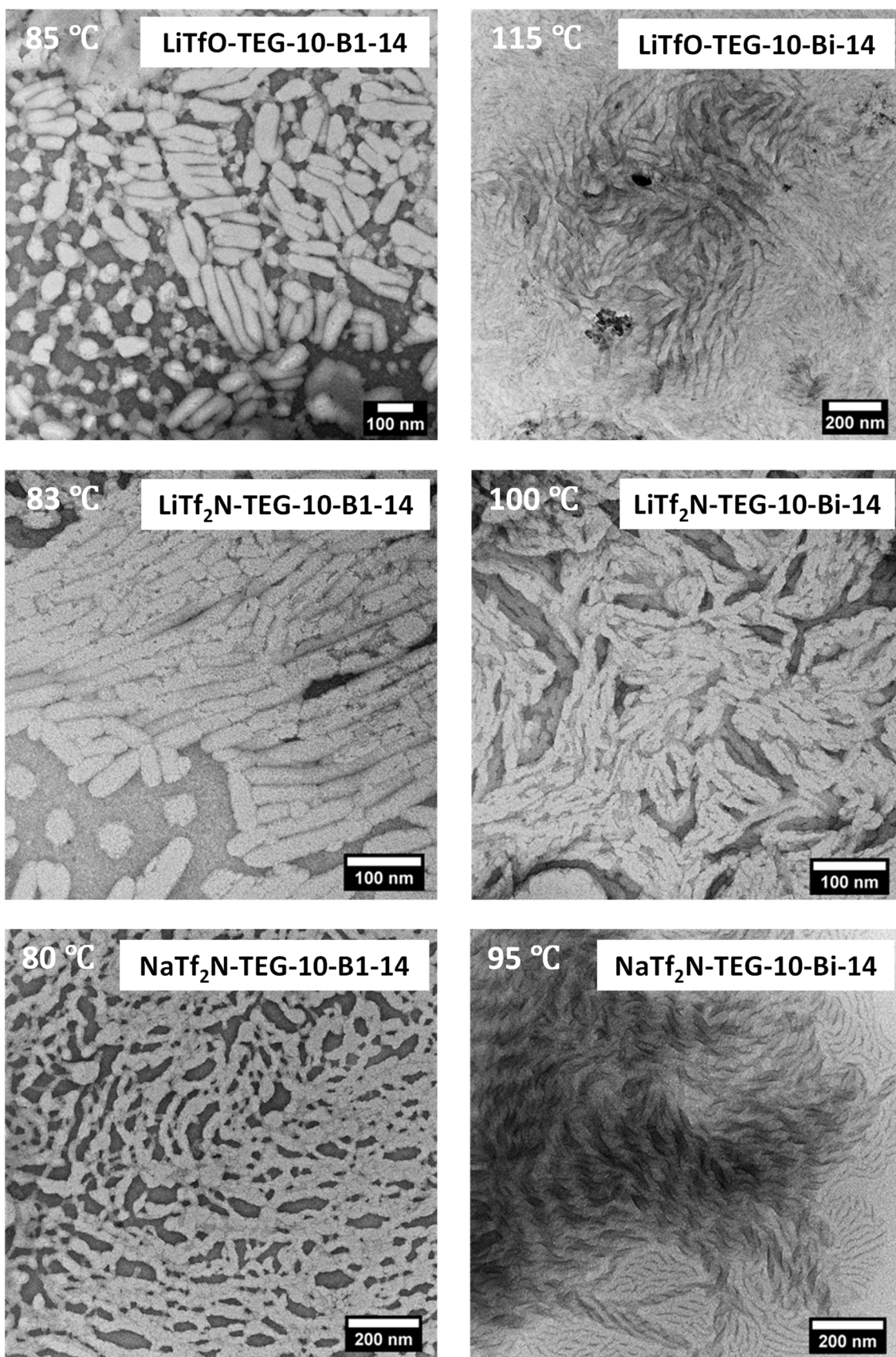


Figure S11. TEM images of MA-TEG-10-Bx-14 complexes (based on the B1-core, left; and the Bi-core, right) obtained after heating the samples to the isotropic liquid phase and subsequent quenching at the liquid crystalline phase, and then studied at room temperature.

- SECTION 55. X-Ray Diffraction Studies.

Our strategy for structure characterization consisted in the construction of electron density maps (Fourier maps) in 1D ($\rho(z)$) for SmCP and HNF-like structures and in 2D ($\rho(x, y)$) for USmCP and Col-Ob ones, using the diffracted intensities after indexing the X-ray diagram. The procedure can be carried out if the symmetry of the structure contains inversion centers or two-fold axes perpendicular to the translation lattice, as is the case of practically the whole set of structural models proposed up to now. In this situation the structure factors are real, their moduli are the square root of the intensities, and only their signs are to be determined. The following expressions result for the electron density apart from an additive constant:⁵

$$\rho(z) = \frac{1}{c} \sum_l \pm \sqrt{I(l)} \cos[2\pi lz],$$

$$\rho(x, y) = \frac{1}{A} \sum_{hk} \pm \sqrt{I(hk)} \cos[2\pi(hx + ky)],$$

being c the lattice spacing and A the cell area. The coordinates x, y, z are expressed in units of the lattice parameters, and $I(l)$ and $I(hk)$ are the intensities once corrected from the geometrical factors that are inherent to our experiment.

The procedure can be carried out if the symmetry of the structure contains inversion centers or two-fold axes perpendicular to the translation lattice, as is the case of practically the whole set of structural models proposed up to now. In this situation the structure factors are real, their moduli are the square root of the intensities, and only their signs are to be determined. It is worth noting that the method has some ambiguity, because the phases (0 or π) of the different Fourier components are not experimentally accessible. As a consequence, more than one map can be compatible with the X-ray pattern of a compound. The correct sign combination is decided by the physical merit of the obtained density map, considering the packing conditions, molecular sizes and optimization of the steric interactions. Finally, a completely reliable image of the structure is obtained by positioning the molecules on the selected map.

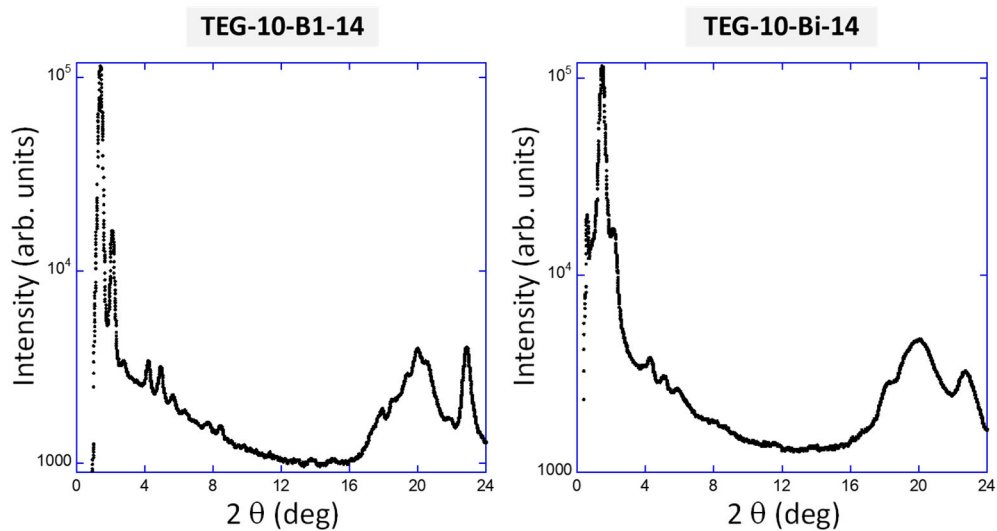


Figure S12. X-ray diagram of compounds: TEG-10-B1-14 at 60 °C and of TEG-10-Bi-14 at 70 °C.

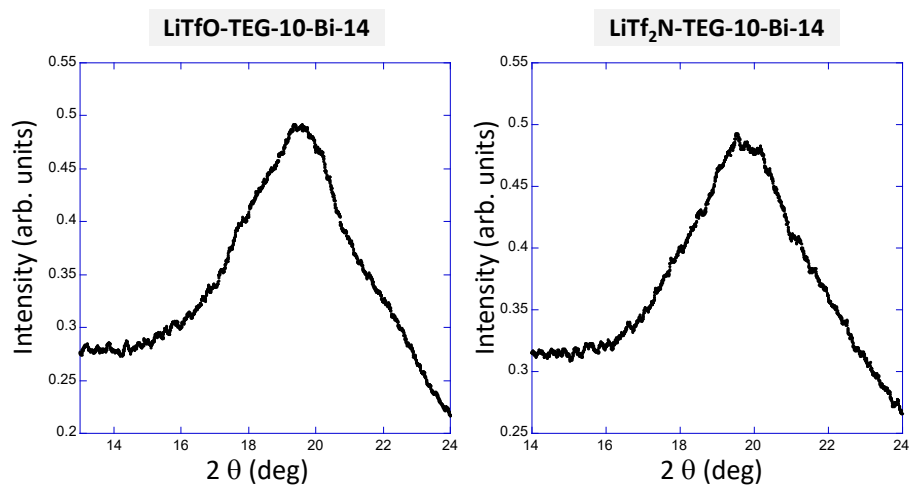


Figure S13. The wide-angle region of the X-ray diagrams of complexes LiTfO-TEG-10-Bi-14 and LiTf₂N-TEG-10-Bi-14 are not the typical one of a liquid crystal phase, showing the contribution of some reflections.

- SECTION S6. Dielectric Studies in bulk materials

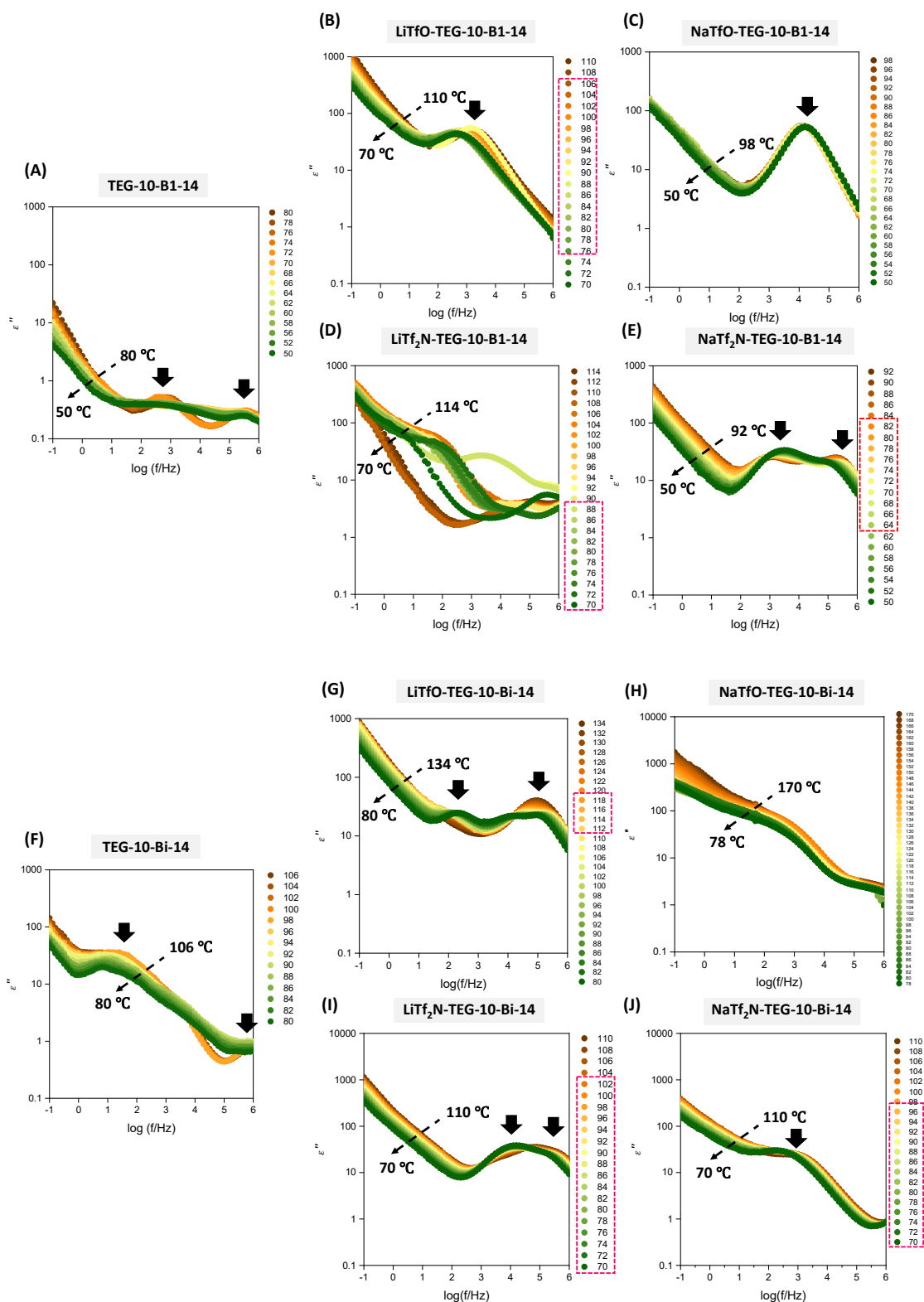


Figure S14. Bode plots showing the frequency and temperature dependence of dielectric loss factor (ϵ'') measured for the non-doped and doped samples of compounds **TEG-10-B1-14** (above) and of **TEG-10-Bi-14** (below), on cooling from the corresponding isotropic melts. Vertical arrow pinpoint dielectric process. Dotted lines indicate the direction on cooling.

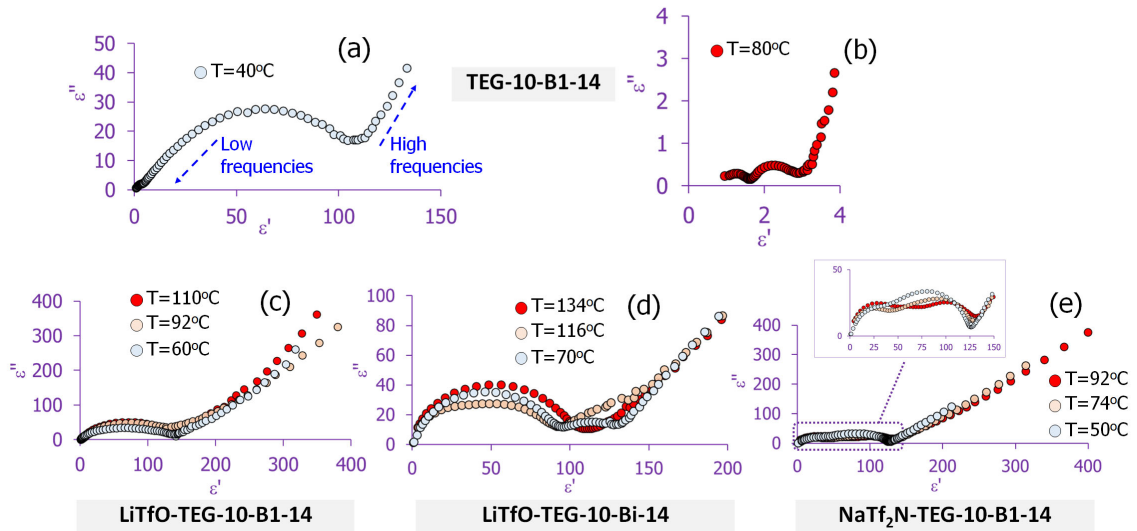


Figure S15. Cole-Cole plots (ϵ'' vs ϵ') obtained from the dielectric/conductivity measurements, for selected samples and conditions: (a) **TEG-10-B1-14** @ $T=40^\circ\text{C}$ (crystal phase); (b) **TEG-10-B1-14** @ $T=80^\circ\text{C}$ (isotropic melt); (c) **LiTFS-TEG-10-B1-14**: @ $T=110^\circ\text{C}$ (isotropic), @ $T=92^\circ\text{C}$ (SmCP), @ $T=60^\circ\text{C}$ (crystal); (d) **LiTFS-TEG-10-Bi-14**: @ $T=134^\circ\text{C}$ (isotropic), @ $T=116^\circ\text{C}$ (HNF-like), @ $T=70^\circ\text{C}$ (crystal); (e) **NaTFSI-TEG-10-B1-14**: @ $T=92^\circ\text{C}$ (isotropic), @ $T=74^\circ\text{C}$ (USmCP), @ $T=50^\circ\text{C}$ (crystal).

- SECTION S7. Self-assembly Studies.

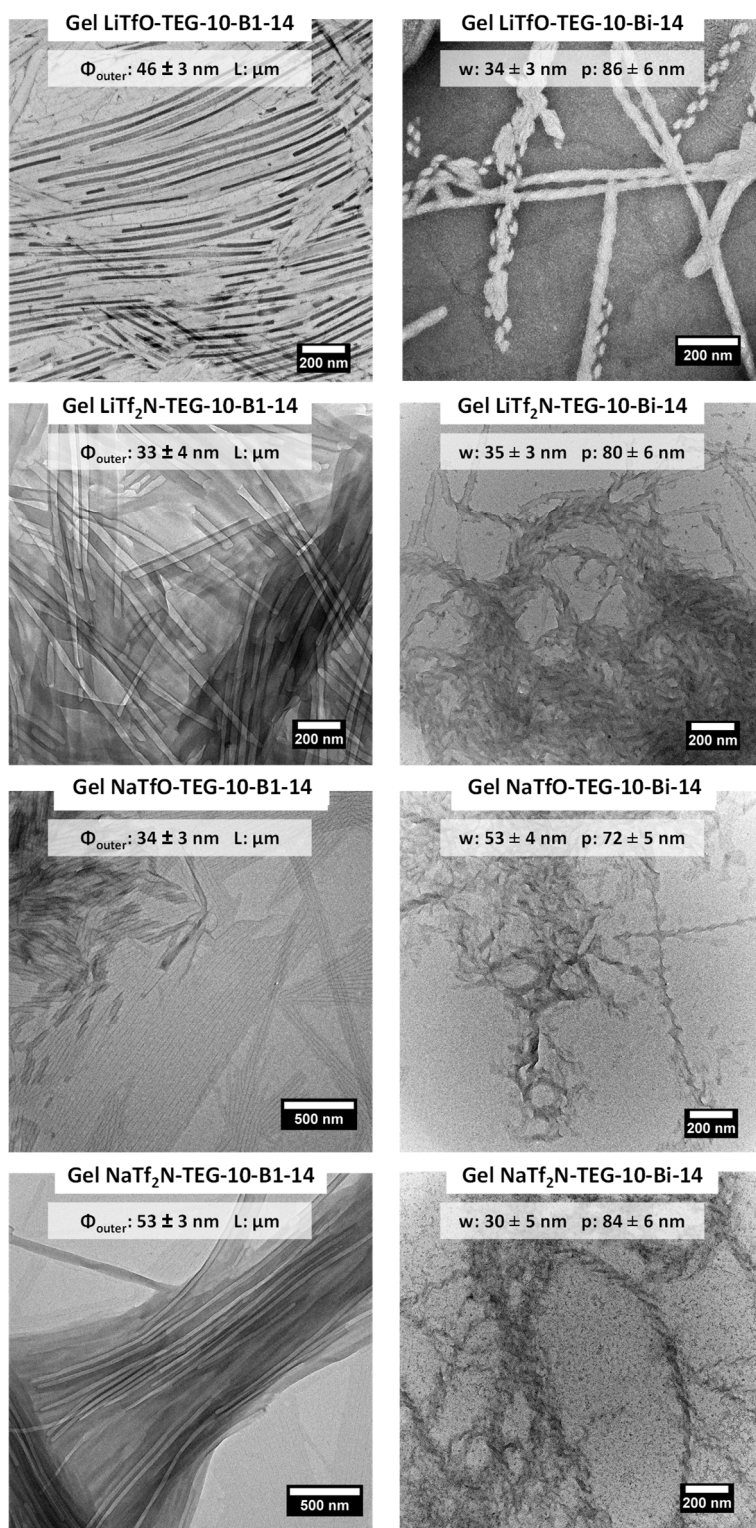


Figure S16. TEM images of gels obtained with at 1 wt% of complexes **MA-TEG-10-B1-14** and **MA-TEG-10-Bi-14** in 1-octanol. Nanotube diameters (Φ_{outer}), widths (w), periodicity of helical arrangements (p), and lengths (L) are indicated in each case.

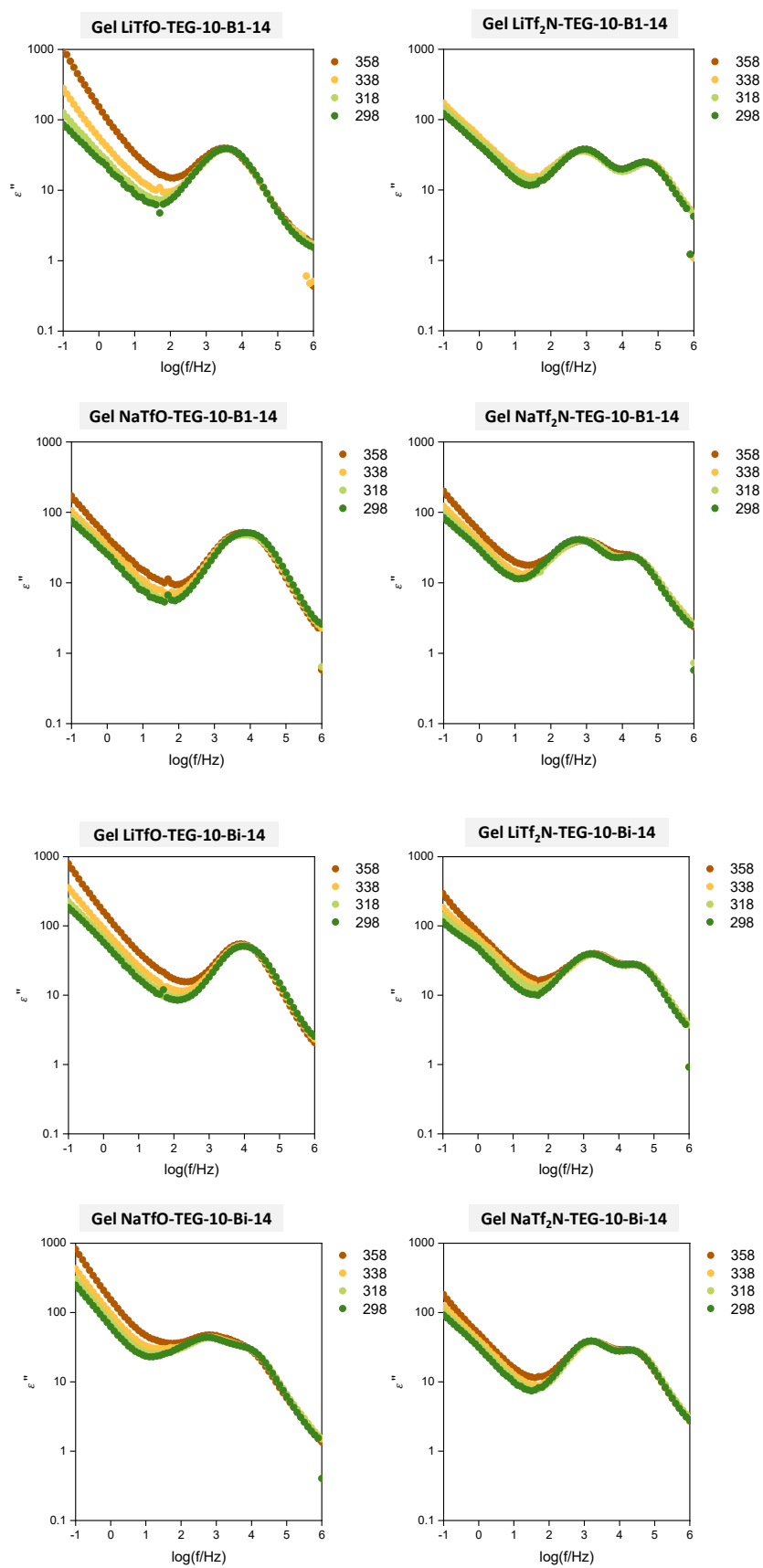


Figure S17. Bode plots showing the frequency and temperature dependence of the dielectric loss factor (ϵ'') measured for gels of 1 wt% of complexes MA-TEG-10-B1-14 and MA-TEG-10-Bi-14 in 1-octanol, on cooling from the corresponding isotropic solutions to gel at room temperature.

REFERENCES

- (1) Gimeno, N.; Pintre, I.; Martínez-Abadía, M.; Serrano, J. L.; Ros, M. B. Bent-Core Liquid Crystal Phases Promoted by Azo-Containing Molecules: From Monomers to Side-Chain Polymers. *RSC Adv* **2014**, *4* (38), 19694–19702.
- (2) Gimeno, N.; Ros, M. B.; Serrano, J. L.; de la Fuente, M. R.; Gimeno, N.; Ros, M. B.; Serrano, J. L.; de la Fuente, M. R. Hydrogen-Bonded Banana Liquid Crystals. *Angewandte Chemie International Edition* **2004**, *43* (39), 5235–5238.
- (3) Tsai, E.; Richardson, J. M.; Korblova, E.; Nakata, M.; Chen, D.; Shen, Y.; Shao, R.; Clark, N. A.; Walba, D. M. A Modulated Helical Nanofilament Phase. *Angewandte Chemie International Edition* **2013**, *52* (20), 5254–5257.
- (4) Kardas, D.; Prehm, M.; Baumeister, U.; Pocięcha, D.; Reddy, R. A.; Mehl, G. H.; Tschierske, C. End Functionalised Liquid Crystalline Bent-Core Molecules and First DAB Derived Dendrimers with Banana Shaped Mesogenic Units. *J Mater Chem* **2005**, *15* (17),
- (5) Folcia, C. L.; Alonso, I.; Ortega, J.; Etxebarria, J.; Pintre, I.; Ros, M. B. Achiral Bent-Core Liquid Crystals with Azo and Azoxy Linkages: Structural and Nonlinear Optical Properties and Photoisomerization. *Chemistry of Materials* **2006**, *18* (19), 4617–4626.